TRIDIRECTIONAL PROTONIC CONDUCTIVITY IN SOFT MATERIALS

Riikka Mäki-Ontto[a], Karin de Moel[b], Evgeny Polushkin[b], Gert Alberda van Ekenstein[b], Gerrit ten Brinke[b], and Olli Ikkala[a]

a Department of Engineering Physics and Mathematics,
Helsinki University of Technology,
FIN-02015 HUT, Espoo, Finland.
E-mail: Olli.Ikkala@hut.fi

b Laboratory of Polymer Chemistry and Materials Science Center,
Dutch Polymer Institute, University of Groningen,
NL- 9747 AG Groningen, The Netherlands.
E-mail: G.ten.Brinke@chem.rug.nl.

TKK Report
TKK-F-A809

2001

ISBN 951-22-5750-5

ISSN 1456-3320

1. INTRODUCTION

Hierarchical polymeric materials i.e. *stucture-within-structure* morphologies have interested people due to their potential as functional materials[1]. In this communication we have constructed an assembly of nanoscale protonically conducting "wires" using hierarchical self-organization of polymeric supramolecules. The supramolecules consist of poly(styrene)-*block*-poly(4-vinyl pyridine), ie. PS-*block*-P4VP, where the latter block forms stochiometric acid-base complex with toluene sulphonic acid (TSA) which is, in turn, stochiometrically hydrogen-bonded with pentadecylphenol (PDP), i.e. PS-*block*-P4VP(TSA)$_{1.0}$(PDP)$_{1.0}$. In an effort to achieve "a monodomain", the local structures are aligned globally by shear flow resulting in conductivity enhancement. Protonic transport is macroscopically tridirectional, being largest along the "wires" both below and above the glass transition. The nanoscale structures thus allow tuning of the protonic conductivity and anisotropy in soft materials where the structures have been globally aligned.

Electroactive polymers range from conjugated polymers [2] to ionically and protonically conducting [3] materials. They allow conceptually new applications, based on the polymeric flexibility, as well their processing and design opportunities. Self-organization involving conducting or conjugated domains has been studied already early, based on block copolymers [4-13] and hairy rods [14-17]. More recently, undoped hairy rods [18, 19] and the corresponding doped hydrogen bonded supramolecules [20] have shown attractive transport properties. For ionic conductivity, solid polymer electrolytes involving Lithium salts have aroused major interest where suppression of the host polymer crystallization increases the conductivity and within this context also block copolymers have been used. [21, 22] More recently, the specific possibilities allowed by nanoscale structures using either block copolymeric, hairy-rod type, or liquid crystalline self-organization have been reported for Li-conductors. [23-29] Finally, in protonic conductors, perfluorinated polymeric sulphonic acids are promising materials [3, 30] where the conductivity is due to proton hopping within adsorbed water. [31, 32] Interesting results have been found for polyelectrolyte surfactant complexes, where a conductivity change from ohmic to non-ohmic is observed.[33, 34] Another major type of protonically conductive polymers consists of acid-base complexes, typically salts of sulphonic-acid containing polymers blended with basic polymers. [35, 36] Specific acid-base complexes are studied in this work.

In protonic conductors, the potential of self-organization within the polymeric host has not been much discussed, although self-organization might allow confinement of the moieties involved in the proton hopping (also water molecules) in tailored and stable nanoscale channels. Previously we reported that polymeric supramolecules (for supramolecules in general, see [37]) could be formed by hydrogen bonding alkyl phenols, such as pentadecyl phenol (PDP), to poly(4-vinyl pyridine) (P4VP) which has been complexed with methane sulphonic acid. [38] Such supramolecules self-organize to form lamellar structures. If the P4VP-chains are further covalently connected to polystyrene (PS) blocks, an additional length scale is introduced rendering lamellar-*within*-lamellar structures. [38] In such materials, a sequence of phase transitions as a function of temperature allows switching of protonic conductivity.

In this report, we will construct protonically conducting acid-base complexes forming self-organized polydomain nanostructures, manipulate the structures by flow [39-43] aiming at a monodomain structure, and show that the macroscopically aligned nanostructure with less domain boundaries is directly reflected in the transport of protons, leading to a considerable improved conductivity and to tridirectionality of the macroscopic conductivity anisotropy.

2. EXPERIMENTAL

2.1. Materials and sample preparation.

Poly (4-vinyl pyridine), P4VP was obtained from Polyscience Inc. with M_n = 50 000 g/mol. Polystyrene-*block*-Poly(4-vinyl pyridine), PS(40.0k)-*block*-P4VP(5.6k), was obtained from Polyscience Inc. with polydispersity 1.09. 3-*n*-pentadecylphenol, PDP, was purchased from Aldrich (purity 98 %). It was twice recrystallized with pethrol ether and dried at 40 °C in vacuum for 4 days. Toluene sulphonic acid (TSA) was obtained from Acros (purity 98%) A lamellar-*within*-lamellar structure was obtained by dissolving PS-*b*-P4VP in analysis grade dimethylformamide (DMF) at 60 °C. A stoichiometric amount (with respect to the number of pyridine groups) of PDP and TSA was added to the dilute solution (1 - 2 w%). At the end, DMF was evaporated and the sample was vacuum dried at 80 °C. in vacuum 0.04mbar for 24 h and stored in desiccator. Other details of sample preparation have been described elsewhere, also describing the preparation of the sample pills for the rheology.[41]

2.2. Dynamic Rheology

Oscillatory shear flow using a dynamic rheometer TA Instruments R1000N with cone and plate geometry is used (diameter 20 mm, cone angle 4°). First the samples were shortly heated to 130 °C to obtain a homogenous sample with good contact with the rotor and the stator of the rheometer. Oscillatory shear flow parameters were chosen in agreement with previous work on PS-*b*-P4VP(PDP)$_{1.0}$[41, 53]. After imposing shear flow, the samples were cooled below 0° with liquid nitrogen and removed from the rheometer.

2.3. Small Angle X-Ray Scattering

The resulting structure was inspected with SAXS device Bruker NanoSTAR: a ceramic fine-focus X-ray tube is used in a point focus mode. The tube is powered with a Kristalloflex K760 generator at 35 kV and 40 mA. The primary beam is collimated with cross-coupled Göbel mirrors and a pinhole of 0.1 mm in diameter providing a CuKa radiation beam (l = 1.54 Å) with a full-width half-maximum about 0.2 mm at the sample position. The sample-detector distance was varied from 0.64 to 1.08m. Using a Hi-Star position-sensitive area detector (Siemens-AXS) allowed recording the scattering intensity in the q-range 0.08 to 3 nm^{-1}.

2.4. Conductivity measurements

The conductivities were studied using HP4192LF Impedance Analyzer at frequencies 10 Hz –10 MHz. The P4VP(TSA)$_{1.0}$ and PS-*block*- P4VP(TSA)$_{1.0}$PDP$_{1.0}$ were dried before measurement at 60 °C for 24 hours at 4 x 10^{-2} mbar and afterwards stored in dry atmosphere. In the measurement setup the sample (typical size ca. 1 x 1 x 2 mm^3) was placed between two platinum plates. The sample was surrounded with teflon in order to isolate the material from atmospheric humidity and reduce development of defects while measuring above T_g of the material.

The complex impedance plot (resistance vs. reactance) showed typical semicircle behavior. The conductivity of the sample was determined based on the intermediate frequency plateau, i.e. near 1 kHz, where the electrode interface polarization does not play a major role, for examples, see the inset of Fig 5A.

For the temperature sweep, a modified Linkam TMS 91 was used with heating and cooling rate of 1°/minute first from 60 °C to 115 °C and another cycle to 140°C for PS-*block*-P4VP(TSA)$_{1.0}$PDP$_{1.0}$. For P4VP(TSA)$_{1.0}$PDP$_{1.0}$ the heating cycle was first 1°/minute first from 50 °C to 110 °C and another cycle from 60 °C to 170°C which is well above the T_{ODT}. With P4VP(TSA)$_{1.0}$ salt the heating cycle was from 60 °C to 170°C.

3. RESULTS AND DISCUSSION

An acid-base complex is formed between P4VP and a stoichiometric amount of toluene sulphonic acid (TSA). This choice was motivated by two factors: Firstly, the acid-base complexes between several basic polymers, including P4VP, with polymeric sulphonic acids allow relatively high protonic conductivity both in the hydrated and dehydrated state. [35, 36] In this work, we preferred oligomeric sulphonic acids, as we expected more perfect structures in this case. Secondly, TSA was selected because its aromatic nature allows enhanced thermal stability. A stoichiometric amount of PDP *vs.* sulphonate groups was taken to form the hydrogen bonded comb-shaped complex (Scheme 1). The above P4VP was selected to be one block of a diblock copolymer PS-*block*-P4VP with weight fraction of PS f_{PS} = 0.88. Assuming that TSA and PDP are nominally fully complexed to form the supramolecules PS-*block*-P4VP(TSA)$_{1.0}$(PDP)$_{1.0}$(Scheme 1), the weight fraction of the PS block is f_{PS} = 0.62. It suggests self-organized alternating lamellae of PS and P4VP(TSA)$_{1.0}$(PDP)$_{1.0}$ (see also [38, 44] for

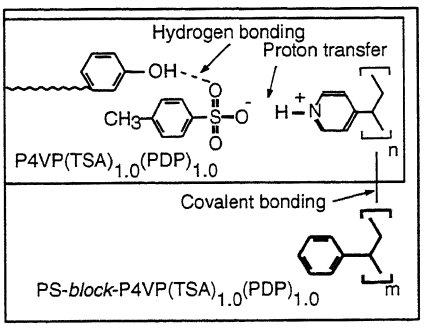

Scheme 1

related materials). Our previous studies [38, 44] suggest that within the P4VP(TSA)$_{1.0}$(PDP)$_{1.0}$ layers, there will be another, i.e. "inner", level of self-organization which consists of alternating layers of nonpolar pentadecyl chains and polymeric salt moities. The expected scheme of self-organization is shown in Fig. 1B. That such structures really were achieved will be demonstrated later by small angle X-ray scattering (SAXS), see Fig. 2.

The self-organized nanoscale structures are local structures and additional driving forces, such as flow field [39, 40, 42, 43], electric field [45], or surfaces [46] have to be invoked to

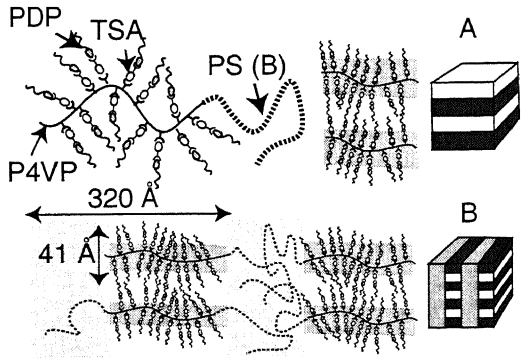

Fig 1. Schematics of the self-organized structures based on the acid-base protonic conductor P4VP(TSA)$_{1.0}$. A) P4VP(TSA)$_{1.0}$(PDP)$_{1.0}$: 2-dimensional (lamellar) nanoscale conducting lamellae upon hydrogen bonding to pentadecyl phenol (PDP). B) PS-*block*-P4VP(TSA)$_{1.0}$(PDP)$_{1.0}$: Essentially 1-dimensional protonically conducting nanoscale wires. The hierarchical self-organization due to covalent connection between P4VP and polystyrene (PS) to form block copolymer and hydrogen bonding of P4VP(TSA)$_{1.0}$ to PDP are indicated.

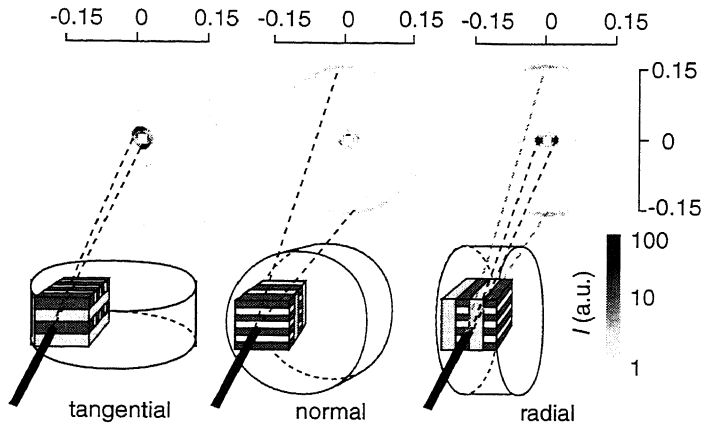

Fig 2. Flow-induced overall alignment of the protonically conducting nanoscale wires of PS-*block*-P4VP(TSA)$_{1.0}$PDP$_{1.0}$ after shearing at 0.1 Hz, 100 % strain amplitude at 140 °C and 110 °C both for 8 hours. The corresponding 2-dimensional SAXS intensities in the tangential, normal, and radial directions are shown. The scale is in Å^{-1}.

achieve macroscopic alignment when striving towards monodomains. Fig. 2 shows the 2-dimensional SAXS intensity patterns of a flow oriented sample in the tangential, normal, and radial directions. Scattering peaks are observed at $q_1 = 0.02$ Å^{-1} and $2q_1$ which demonstrates a lamellar self-organization between PS and P4VP(TSA)$_{1.0}$(PDP)$_{1.0}$ with a periodicity of 320 Å. The lamellae are relatively well aligned along the shearing planes, see Fig. 2. SAXS shows also another peak at $q_2 = 0.15$ Å^{-1}. The second order peak is beyond the range shown of Fig 2. However, from the corresponding homopolymeric supramolecules P4VP(TSA)$_{1.0}$(PDP)$_{1.0}$ (see Fig. 4) the structure can be assigned to a lamellar order with a long period of 41 Å. The net

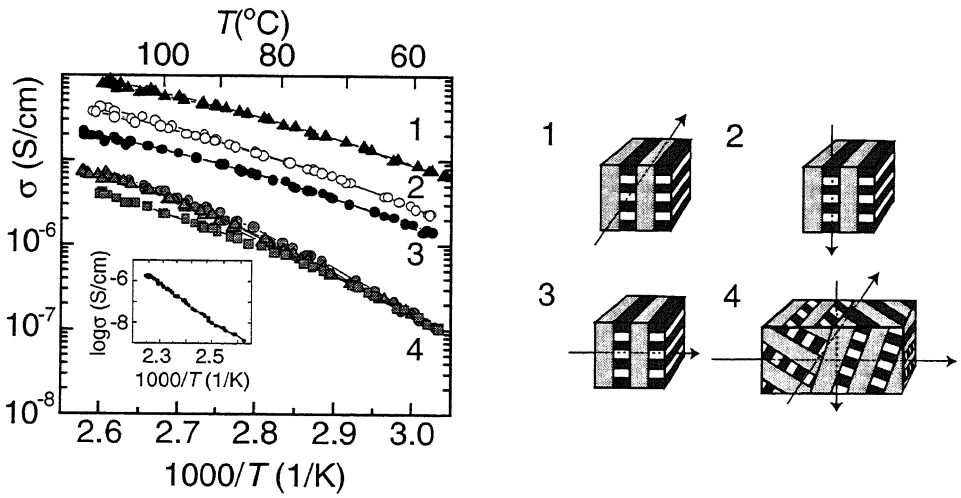

Fig 3. DC-conductivity of PS-*block*-P4VP(TSA)$_{1.0}$PDP$_{1.0}$ as a function of temperature. The inset shows the conductivity of the pristine P4VP(TSA)$_{1.0}$ which is poor due to crystallinity. In the non-aligned case (gray symbols, case 4), the protonic conductivity is improved and isotropic due to the polydomain structure with different local orientations of the conducting nanowires. In the aligned case (solid and open symbols, cases 1, 2, and 3), the protonically conducting nanowires have overall orientation due to the nearly monodomain structure. The conductivity is still increased obviously due to fewer domains boundaries and the nanoscale conductivity anisotropy is manifestly present.

structure is shown in Fig. 1B. Importantly, this structure, corresponding to the orientation of the protonically conducting nanowires, becomes globally relatively well oriented after the imposed flow, as shown in Fig. 2.

The conductivities were investigated using the simple Arrhenius and empirical Vogel-Tamman-Fulcher (VTF) equations, which are widely used for crystalline and amorphous polymer electrolytes [47-50]. The inset of Fig. 3 shows the conductivity of pristine acid-base complex P4VP(TSA)$_{1.0}$. The conductivity is poor and obeys the Arrhenius equation, $\sigma(T) = A\exp(-E_\sigma/kT)$ with the activation energy $E_\sigma \approx 1.8$ eV. Fig 3 shows that the conductivity of PS-*block*-P4VP(TSA)$_{1.0}$PDP$_{1.0}$ is drastically higher due to plasticization, even without alignment. The empirical VTF equation $\sigma(T) = A/T^{1/2}\exp[-E_a/(k(T-T_0))]$ describes its conductivity, with a pseudo activation energy $E_a \approx 0.10$ eV and a characteristic temperature $T_0 = -74$ °C, which is typically related to the glass transition temperature. In the non-aligned case the conductivity is isotropic in all three dimensions with $E_a \approx 0.15$ eV as the local anisotropies have been averaged out due to the polydomain structure. Interestingly, Fig. 3 further shows that upon macroscopic alignment, the conductivities in the three directions still increase, possibly due to enhancement of organization of nanostructure and reduction of domain boundaries. The conductivity is anisotropic with the conductivity being highest along the macroscopically aligned protonically conducting nanoscale wires. Lower values are observed for the direction across the relatively thin (order of magnitude: 20 Å) insulating pentadecyl layers. The lowest values, however, are observed in the direction across the relatively thick PS layers (order of magnitude: 150 Å). This is in good agreement with the structural information from SAXS (Fig. 3).

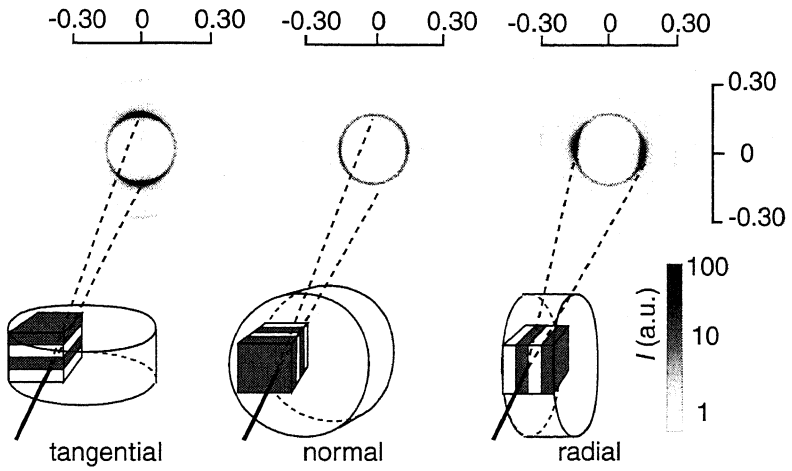

Fig 4. The flow-induced overall alignment of the protonically conducting lamellae of P4VP(TSA)$_{1.0}$PDP$_{1.0}$ after shearing at 0.1 Hz, 100% strain amplitude at 110 °C for 8 hours. The corresponding 2-dimensional SAXS intensities in the tangential, normal, and radial directions are shown. The scale is in Å^{-1}.

In order to analyze the protonic hopping transport in more detail, it is helpful first to consider the homopolymeric supramolecules P4VP(TSA)$_{1.0}$PDP$_{1.0}$. This material was also oriented by shear flow and characterized using SAXS, see Fig. 4. Peaks at $q_2 = 0.15$ Å^{-1} and $2q_2$ indicate lamellar order with a periodicity of 41 Å, see also Fig. 1A. Fig. 4 further shows that the conducting lamellae are well oriented along the shearing planes. Also in this case the conductivity is drastically improved in comparison with the pristine P4VP(TSA)$_{1.0}$, e.g. at 80 °C the conductivities along the two lamellar directions were 8 x 10^{-4} S/cm and slightly lower 3 x 10^{-4} S/cm across the insulating pentadecyl layers. The conduction activation energies for P4VP(TSA)$_{1.0}$PDP$_{1.0}$ and PS-*block*-P4VP(TSA)$_{1.0}$PDP$_{1.0}$ are comparable. Finally, the hopping

rates $\omega_p$were evaluated by applying the scaling law $\sigma(\omega) = \sigma(0) + A\omega^n$ [51] to the higher frequency data, see the insets of Figs. 5 A and 5 B. The hopping rates of the mobile species were evaluated using $\omega_p = [\sigma(0)/A]^{1/n}$[52], see Fig. 5 A. For P4VP(TSA)$_{1.0}$(PDP)$_{1.0}$, the hopping rates along the protonically conducting nanoscale layers are an order of magnitude larger than across the pentadecyl insulating layer, see Fig. 5 A. In agreement, in PS-*block*-P4VP(TSA)$_{1.0}$PDP$_{1.0}$ the hopping rate is decreased roughly an order of magnitude across the thin pentadecyl layers and still another order of magnitude across the thicker PS layers, see Fig. 5 B. Therefore, the local tridirectional anisotropy of the nanostructures is directly reflected in the macroscopic conductivity.

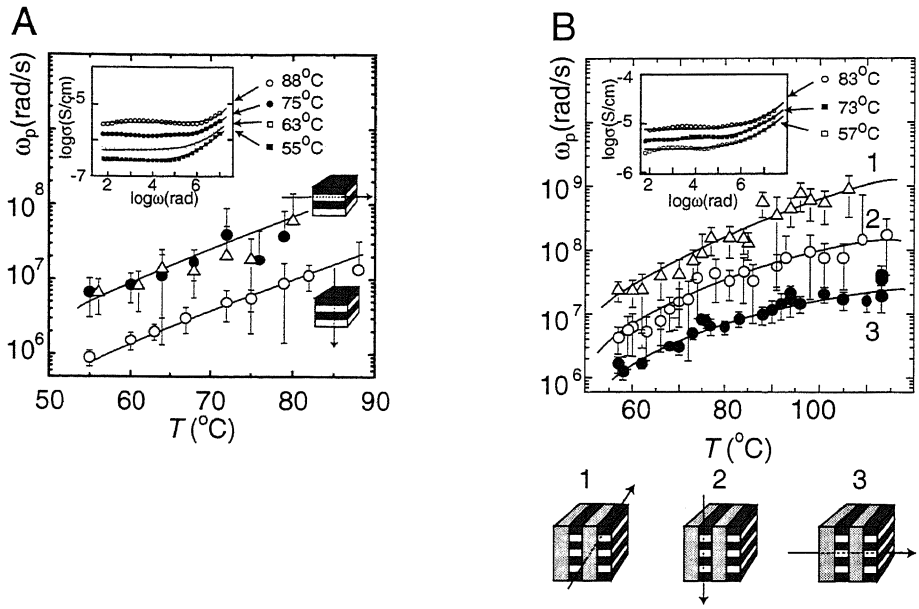

Fig 5. Hopping rates for the protonic conductivity. A) For P4VP(TSA)$_{1.0}$(PDP)$_{1.0}$ the hopping rate within the nanoscale lamellae consisting of P4VP(TSA)$_{1.0}$ is an order of magnitude larger than across the thin pentadecyl alkyl layers. B) For PS-*block*-P4VP(TSA)$_{1.0}$(PDP)$_{1.0}$, similarly, the largest hopping rate is observed along the nanoscale wires (Δ, case 1). The hopping rate is an order of magnitude reduced across the insulating pentadecyl alkyl layers (O, case 2) and still another ca. order of magnitude less into the third direction where the hopping should take across the thick polystyrene layers (●, case 3).

4. CONCLUSION

In conclusion, specific acid-base supramolecules were constructed and the presence of attractive and repulsive interactions renders local nanoscale conducting domains due to self-organization. The number of domain boundaries, i.e. defects, can be reduced by macroscopic alignment of the local nanostructures, which in this work has been accomplished by an imposed flow. Plasticized materials with improved protonic conduction were obtained. The nanoscale structures allow tuning of the protonic transport: two-dimensional nanostructures provide conductivity anisotropy in two dimensions, and three-dimensional nanostructures in three dimensions. Thus the molecular level anisotropy reflects in the macroscopic conductivity behavior in a controlled way.

ACKNOWLEDGEMENTS

The work has been supported by Finnish Academy and Technology Development Centre (Finland). K. de M. gratefully acknowledges financial support from DSM within the Computational Materials Science program of the Dutch Society for Scientific research (NWO). Tapio Mäkelä is acknowledged for instruction in the electrical measurements.

REFERENCES

[1] M. Muthukumar, C. K. Ober, E. L. Thomas, *Science* **1997**, *277*, 1225.
[2] T. A. Skotheim, R. L. Elsenbaumer, J. R. Reynolds, in *Handbook of Conducting Polymers* (Ed: Marcel Dekker, Inc., New York **1998**
[3] F. M. Gray, *Polymer Electrolytes,* VCH Publishers, Weinheim, **1991**.
[4] R. I. Stankovic, R. W. Lenz, F. E. Karasz, *Eur. Polym. J.* **1990**, *26*, 359.
[5] R. I. Stankovic, R. W. Lenz, F. E. Karasz, *Eur. Polym. J.* **1990**, *26*, 675.
[6] S. Kempf, H. W. Rotter, S. N. Magonov, W. Gronski, H. J. Cantow, *Polym. Bull. (Berlin)* **1990**, *24(3)*, 325.
[7] S. Kempf, W. Gronski, *Polymer Bulletin* **1990**, *23*, 403.
[8] K. Ishizu, Y. Yamada, R. Saito, T. Yamamoto, T. Kanbara, *Polymer* **1992**, *33*, 1816.
[9] K. Ishizu, Y. Yamada, R. Saito, T. Kanbara, T. Yamamoto, *Polymer* **1993**, *34*, 2256.
[10] K. Ishizu, K. Honda, T. Kanbara, T. Yamamoto, *Polymer* **1994**, *35(22)*, 4901.
[11] J. Li, I. M. Khan, *Makromol. Chem.* **1991**, *192*, 3043.
[12] L. Dai, J. W. White, *Polymer* **1997**, *38*, 775.
[13] B. H. Sohn, R. E. Cohen, *J. of Appl. Polym. Sci.* **1997**, *65*, 723.
[14] K. Yoshino, S. Nakajima, R.-I. Sugimoto, *Jpn. J. Appl.Phys.* **1987**, *6*, L2046.
[15] T. J. Prosa, M. J. Winokur, J. Moulton, P. Smith, A. J. Heeger, *Macromolecules* **1992**, *25*, 4364.
[16] G. Wegner, *Makromol. Chem., Macromol. Symp.* **1986**, *1*, 151.
[17] T. Vahlenkamp, G. Wegner, *Makromol. Chem. Phys.* **1994**, *195*, 1933.
[18] H. Sirringhaus, P. Brown, R. H. Friend, M. M. Nielsen, K. Becgaard, B. M. W. Langeveld-Voss, A. J. H. Spiering, R. A. J. Janssen, E. W. Meijer, P. Herwig, D. M. de Leeuw, *Nature* **1999**, *401*, 685.
[19] J. H. Schön, A. Dodabalapur, Z. Bao, C. Kloc, O. Schenker, B. Batlogg, *Nature* **2001**, *410*, 189.
[20] H. Kosonen, J. Ruokolainen, M. Knaapila, M. Torkkeli, K. Jokela, R. Serimaa, G. ten Brinke, W. Bras, A. P. Monkman, O. Ikkala, *Macromolecules* **2000**, *33*, 8671.
[21] J. R. M. Giles, F. M. Gray, J. R. MacCallum, C. A. Vincent, *Polymer* **1987**, *28*, 1977.
[22] P. Lobitz, H. Fuellbier, A. Reiche, J. C. Illner, H. Reuter, S. Hoering, *Solid State Ionics* **1992**, *58*, 41.
[23] I. M. Khan, D. Fish, Y. Delaviz, J. Smid, *Makromol. Chem.* **1989**, *190*, 1069.
[24] P. V. Wright, Y. Zheng, D. Bhatt, T. Richardson, G. Ungar, *Polymer International* **1998**, *47*, 34.
[25] P. P. Soo, B. Huang, Y.-I. Jang, Y.-M. Chiang, D. R. Sadoway, A. M. Mayers, *J. of Electrochem. Soc.* **1999**, *146*, 32.
[26] U. Lauter, W. H. Meyer, G. Wegner, *Macromolecules* **1997**, *30*, 2092.
[27] T. Ohtake, M. Ogasawara, K. Ito-Akita, N. Nishina, S. Ujiie, H. Ohno, T. Kato, *Chem. Mater.* **2000**, *12*, 782.
[28] T. Ohtake, Y. Takamitsu, M. Ogasawara, K. Ito-Akita, K. Kanie, M. Yoshizawa, T. Mukai, H. Ohno, T. Kato, *Macromolecules* **2000**, *33*, 8109.
[29] A.-V. Ruzette, P. Soo, D. Sadoway, A. Mayes, *J. of Electrochem. Soc.* **2001**, *146*, A537.
[30] K. D. Kreuer, *Chem. Mater.* **2000**, *8*, 610.
[31] N. Agmon, *Chem. Phys. Letters* **1995**, *244*, 456.
[32] M. Eikerling, A. A. Kornyshev, A. M. Kuznetsov, J. Ulstrup, S. Walbran, *J. Phys. Chem. B* **2001**, *105*, 3646.
[33] M. Antonietti, M. Neese, G. Blum, F. Kremer, *Langmuir* **1996**, *12*, 4436.
[34] M. Antonietti, M. Maskos, F. Kremer, G. Blum, *Acta Polymer* **1996**, *47*, 460.
[35] J. Kerres, A. Ullrich, F. Meier, T. Haring, *Solid State Ionics* **1999**, *125*, 243.
[36] M. Rikukawa, K. Sanui, *Prog. Polym. Sci.* **2000**, *25(10)*, 1463.
[37] J.-M. Lehn, *Supramolecular Chemistry,* VCH, Weinheim, **1995**.
[38] J. Ruokolainen, R. Mäkinen, M. Torkkeli, R. Serimaa, T. Mäkelä, G. ten Brinke, O. Ikkala, *Science*

1998, *280*, 557.
[39] Z.-R. Chen, J. A. Kornfield, S. D. Smith, J. T. Grothaus, M. M. Satkowski, *Science* **1997**, *277*, 1248.
[40] J. Sänger, W. Gronski, H. Leist, U. Wiesner, *Macromolecules* **1997**, *30*, 7621.
[41] R. Mäkinen, J. Ruokolainen, O. Ikkala, K. de Moel, G. ten Brinke, W. De Odorico, M. Stamm, *Macromolecules* **2000**, *33*, 3441.
[42] G. Hadziioannou, A. Mathis, A. Skoulios, *Colloid & Polymer Science* **1979**, *257*, 136.
[43] K. A. Koppi, M. Tirrell, F. S. Bates, *J. Phys. II France* **1992**, *2*, 1941.
[44] J. Ruokolainen, G. ten Brinke, O. T. Ikkala, *Adv. Mat.* **1999**, *11*, 777.
[45] T. Thurn-Albrecht, R. Steiner, J. DeRouchey, C. M. Stafford, E. Huang, M. Bal, M. Tuominen, C. J. Hawker, T. P. Russell, *Adv. Mat.* **2000**, *12*, 787.
[46] K. Ishizu, T. Fukuyama, *Macromolecules* **1989**, *22*, 244.
[47] W. Wieczorek, S. H. Chung, J. R. Stevens, *J. of Polym. Sci., Part B: Polym. Phys.* **1996**, *34*, 2911.
[48] N. Binesh, S. V. Bhat, *J. of Polym. Sci., Part B: Polym. Phys.* **1998**, *25*, 1201.
[49] S. H. Chung, K. Such, W. Wieczorek, J. R. Stevens, *J. Polym. Sci., Part B: Polym. Phys.* **1994**, *32*, 2733.
[50] M. J. C. Plancha, C. M. Rangel, C. A. C. Sequeira, *Solid State Ionics* **1992**, *58*, 3.
[51] K. A. Jonscher, *Nature* **1977**, *267*, 673.
[52] D. P. Almond, G. K. Duncan, A. R. West, *Solid State Ionics* **1983**, *8*, 159.
[53] R. Mäki-Ontto, K. de Moel, W. de Odorico, J. Ruokolainen, M. Stamm, G. ten Brinke, O. Ikkala, *Adv. Mat.* **2001**, *13*, 117.